Published in final edited form as:
Histol Histopathol. 2013 October ; 28(10): 1325–1336.

The effect of low and high plasma levels of insulin-like growth factor-1 (IGF-1) on the morphology of major organs: studies of Laron dwarf and bovine growth hormone transgenic (bGHTg) mice

Katarzyna Piotrowska[1], **Sylwia J. Borkowska**[1], **Barbara Wiszniewska**[2], **Maria Laszczyńska**[3], **Sylwia Słuczanowska-Głąbowska**[1], **Aaron M. Havens**[5], **John J. Kopchick**[6], **Andrzej Bartke**[7], **Russel S. Taichman**[5], **Magda Kucia**[4], and **Mariusz Z. Ratajczak**[1,4]

[1]Department of Physiology Pomeranian Medical University, Szczecin, Poland [2]Department of Histology and Embryology Pomeranian Medical University, Szczecin, Poland [3]Department of Histology and Developmental Biology, Pomeranian Medical University Szczecin, Poland [4]Stem Cell Institute at James Graham Brown Cancer Center, University of Louisville, USA [5]Periodontics and Oral Medicine, University of Michigan, Ann Arbor, MI, United States [6]Edison Biotechnology Institute and Department of Biomedical Sciences, College of Osteopathic Medicine, Ohio University, Athens, OH, USA [7]Geriatrics Research, Departments of Internal Medicine and Physiology, Southern Illinois University School of Medicine, Springfield, IL, USA

Summary

It is well known that somatotrophic/insulin signaling affects lifespan in experimental animals. To study the effects of insulin-like growth factor-1 (IGF-1) plasma level on the morphology of major organs, we analyzed lung, heart, liver, kidney, bone marrow, and spleen isolated from 2-year-old growth hormone receptor knockout (GHR-KO) Laron dwarf mice (with low circulating plasma levels of IGF-1) and 6-month-old bovine growth hormone transgenic (bGHTg) mice (with high circulating plasma levels of IGF-1). The ages of the two mutant strains employed in our studies were selected based on their overall ~50% survival (Laron dwarf mice live up to ~4 years and bGHTg mice up to ~1 year). Morphological analysis of the organs of long-living 2-year-old Laron dwarf mice revealed a lower biological age for their organs compared with normal littermates, with more brown adipose tissue (BAT) surrounding the main body organs, lower levels of steatosis in liver, and a lower incidence of leukocyte infiltration in different organs. By contrast, the organs of 6-month-old, short-living bGHTg mice displayed several abnormalities in liver and kidney and a reduced content of BAT around vital organs.

Keywords

Aging; Brown adipose tissue; Insulin-like growth factor-1 (IGF-1); Growth hormone (GH); Laron dwarf mice

Offprint requests to: Mariusz Z. Ratajczak MD, PhD, Hoenig Endowed Chair, Professor and Director Stem Cell Institute at James Graham Brown Cancer Center, University of Louisville, 500 S. Floyd Street, Rm. 107, Louisville, KY 40202, USA. mzrata01@louisville.edu.

Introduction

Risk factors such as obesity, diabetes, high caloric consumption and lack of physical activity, lead to atherosclerosis of the cardio-vascular system and cancer, impair the function of vital organs, and limit overall life span (Fontana et al., 2008; Piper and Bartke 2008; Ikeno et al., 2009). All these risk factors are directly or indirectly related to prolonged insulin/insulin-like growth factor signaling (IIS) and must ultimately have an impact on tissue rejuvenation (Kucia et al., 2013). In particular, the plasma level of insulin-like growth factor-1 (IGF-1) inversely correlates with life span in experimental animals (Bartke, 2008). To evaluate the effect of IGF-1 plasma level on the morphology of major organs, we focused on two mouse models which express different levels of IGF-1 which impact the life span of the mouse strains including the i) long- living Laron dwarf mice, which have very low levels of plasma IGF-1, and ii) short-living mice that overexpress bovine growth hormone (bGH), which have elevated plasma levels of IGF-1 (Zhou et al., 1997; Olsson et al., 2003).

Long-living Laron dwarf mice have a deletion of the GH receptor/GH-binding protein gene (GHR-KO) that makes them insensitive to GH signaling. As a result of GH resistance, these mice have reduced plasma levels of circulating IGF-1 and insulin, with simultaneously elevated GH levels. They live for up to 4 years, are smaller than normal littermates, and display enhanced insulin sensitivity and normal or slightly decreased glucose levels in blood (Gesing et al., 2011). Furthermore, recent results show that GHR-KO mice, like other murine strains with disruption of the GH/IGF-1 axis, are more resistant to cancer development (Clayton et al., 2011), and fibroblastic cell lines derived from these mice are more resistant to stress (Salmon et al., 2005; Harper et al., 2007). Extended life span in these mice correlates with better overall health status in advanced age compared with wild type (WT) animals. Moreover, Laron dwarf mice display better long-term memory (Kinney et al., 2001) and delayed immune and collagen aging (Flurkey et al., 2001). Female GHR-KO mice show prolonged ovulation compared with WT animals and may become pregnant at advanced age, as recently reported (Sluczanowska-Glabowska et al., 2012).

The second strain employed in our studies overexpress bovine growth hormone (bGH) under control of the phosphoenolpyruvatecarboxykinase (PEPCK) promoter. These mice live ~1 year, which is ~50% shorter than control littermates that lack this transgene. High plasma levels of bGH in these animals results in increased blood plasma IGF-1 level. Due to the high levels of GH, these mice display increased body mass, hyperplasia, and hypertrophy of several organs including liver (Bartke et al., 2002; Miquet et al., 2008). Other characteristic features of these animals are low adipose tissue content and insulin resistance (Palmer et al., 2009). These animals also share some features with acromegalic human patients including hypertension, hyperinsulinemia, endothelial dysfunction and kidney glomerulosclerosis (Bartke et al., 2002).

Aging of the tissues and organs is characterized by several morphological features. The most common include; i) tranformation of organ-associated brown adipose tissue (BAT) into white adipose tissue (WAT), ii) nuclear enlargement in hepatocytes, iii) the presence of fatty

liver, iv) a depletion in germinal cells in the gonads, v) an increase in lipofuscin-containing cells in the testes, and vi) signs of mild inflammation in various organs (Maronpot, 1999).

In our studies we employed both strains of mice at approximately the midpoint of their maximal life span (2-year-old GHR-KO and 6-month-old bGHTg mice) for morphological analysis. We also employed their normal age-matched littermates as controls.

Material and methods

Animals

This study was performed in accordance with the guidelines of the Animal Care and Use Committee of the Southern Illinois University, the Laboratory Animal Care Committee of the University of Louisville School of Medicine, and the Guide for the Care and Use of Laboratory Animals (Department of Health and Human Services, publication no. NIH 86-23).

The experiments were performed on adult (2-year-old) wild type (WT) mice, GH receptor knockout (GHR-KO, Laron) mice, 6-month-old bGHTg mice, and 6-month-old WT mice as control animals. Mice were housed in a room with a photoperiod of 12 h light and 12 h darkness and a temperature of 20°C and were given free access to standard rodent chow and tap water until the animals were sacrificed and the tissues collected.

Laron dwarf GH receptor-binding protein knockout (GHR-KO) mice

Control and GHR-BPKO(also termed Laron) male mice used in this study were produced in our breeding colony by crossing 129Ola/BALB/c $GHR^{+/-}$ animals (generously provided by Dr. J. J. Kopchick) with mice derived from crosses between C57BL/6J and C3H/J strains and maintained as a closed colony with inbreeding minimized by avoiding brother × sister matings. $GHR^{-/-}$ males were mated with heterozygous ($GHR^{+/-}$) females to produce $GHR^{-/-}$ mice (Zhou et al., 1997).

Bovine GH transgenic (bGHTg) mice

Male phosphoenolpyruvatecarboxykinase (PEPCK)-bGHTg male mice and their normal male siblings were originally produced by microinjecting the bGH structural gene fused with the promoter of the rat PEPCK gene into the pronuclei of fertilized mouse eggs (McGrane et al., 1988). The hemizygous Tg mice used in this study were produced by mating GH-Tg males with normal C57BL/6 × C3H F1 hybrid females.

Morphological studies

Hearts, lungs, livers, kidneys, and spleens were fixed in 10% buffered formalin for 24 hours and, after dehydration, embedded in paraffin blocks.

Femurs from 2-year-old mice were fixed in 10% neutral buffered formalin for 24 hours. After fixation, the bones were decalcified in Decal (Decal Corporation, NY, USA) for 24 hours, transferred to 70% ethanol for dehydration, and embedded in paraffin blocks.

Deparaffinized sections of all tissues (3 μm thick) were hydrated and stained with hematoxylin and eosin (Sigma) according to the manufacturer's protocol. Livers and kidneys were stained using the PAS (periodic acid Schiff) method. After staining, sections were dehydrated and immersed in a droplet of mounting medium (Sigma). Images were collected with an Olympus IX81 inverted microscope (Olympus, Germany) with color camera and with CellSens image processing software (Olympus, Germany).

Densitometric analysis of bones

Humeri were harvested and immediately fixed in 10% neutral buffered formalin for 24 hours. Specimens were embedded in 1% agarose and placed in a 19 mm diameter tube and scanned over the entire length of the humerus using a microCT system (μCT100 Scanco Medical, Bassersdorf, Switzerland). Scan settings were: voxel size 16 μm, medium resolution, 70 kVp, 114 μA, 0.5 mm AL filter, and integration time 500 ms. Analysis was performed using the manufacturer's evaluation software, and a fixed global threshold of 28% (280 on a grayscale of 0–1000) for cortical bone and 18% (180 on a grayscale of 0-1000) for trabecular bone was used to segment bone from non-bone. Each bone was individually assessed from a 800 μm region of trabecular bone immediately below the growth plate and a 480 μm cortical slice was analyzed around the midpoint of the humerus. Bone mineral density (BMD), trabecular bone volume and cortical total volume were calculated.

Results

The size of all organs tested from GHR-KO (Laron dwarf) mice were smaller than for WT mice and proportional to their smaller body size (Zhou et al., 1997). As expected, we observed hypertrophy and hyperplasia of all the organs tested in bGHTg mice compared with WT mice of the same age.

Morphology of lung and heart in GHR-KO and bGHTg mice

Lungs and hearts from 2-year-old GHR-KO and bGHTg mice had normal morphology. In the lungs of GHR-KO and WT mice we observed well-developed bronchi, bronchioles with Clara cells and alveoli, and no signs of inflammation (Fig. 1A,B). Similarly, hearts in these animals were normally developed and contained well-developed cardiomyocytes (data not shown).

The main difference observed between normal WT (Fig. 1C) and Laron dwarf mice (Fig. 1D) was the predominance of brown adipose tissue (BAT) near the aorta of Laron mice (Fig. 1D) with less BAT and predominantly white adipose tissue (WAT) near the aorta in WT mice (Fig. 1C). The WAT near the aorta in WT mice was also highly infiltrated by leukocytes (Fig. 1C).

Morphological analysis of lungs in 6-month-old bGHTg mice and normal-aged WT littermates revealed normal structure and well-developed bronchi, bronchioles with Clara cells and alveoli, and no signs of inflammation (Fig. 1E,F). Similarly, hearts in these animals also had normal morphology with well-developed cardiomyocytes (not shown).

In sections of adipose tissue from the aorta we observed that bGHTg mice lack BAT and displayed only WAT with infiltration by leucocytes (Fig. 1H). By contrast, in sections from 6-month-old WT animals, adipose tissue near the aorta contained both WAT and BAT (Fig. 1G).

Liver morphology of GHR-KO and bGHTg mice

The most striking morphological changes were observed in the liver. In PAS-stained sections of normal 2-year-old WT mice, livers exhibited a normal lobular structure, with glycogen stored in the centrilobular zone. Hepatocytes contained both small fat droplets (microvesicles) and large fat droplets (macrovesicles). Large lipid droplets were located in the central part of the cell, the nucleus was located peripherally, and fat-storing cells were located in the middle zone of the hepatic lobules (Fig. 2A,C). Numerous hepatocytes had two nuclei or very large single nuclei that were irregular in shape. We also observed signs of inflammation in proximity to some large vessels (Fig. 2C) as well as single cells with intranuclear inclusions (Fig. 2C). By contrast, the liver sinuses in these animals were well developed, and Kupffer cells were visible.

At the same time, livers from 2-year-old Laron dwarf mice showed a normal structure in the liver lobules, with glycogen (indicated by PAS staining) stored in the centrolobular zone. We observed only a small number of fat-storing cells, most of which were filled with microvesicles (ballooning) (Brunt and Tiniakos, 2010). Only single cells contained large fat vesicles, and even in these cells the lipid droplets were smaller than in the hepatocytes of 2-year-old WT mice (Fig. 2B,D). Like WT mice, liver sinuses and Kupffer cells in Laron dwarf animals were normal and, more importantly, did not exhibit fibrosis or inflammation.

By contrast, in liver sections from bGHTg mice we observed morphological changes in lobules, hypertrophy of hepatocytes, accumulation of glycogen in hepatocytes, and irregular shape and increased volume of the nuclei (Fig. 3A-D) compared with liver sections from age-matched control animals (Fig. 3E,F). At the same time, we also observed massive leukocyte infiltrations and liver sinusoids that contained cells filled with lipofuscin granules. The nuclei of the hepatocytes displayed structural changes and contained PAS-positive inclusions (Fig. 3A,D), while some displayed intranuclear vacuoles (Fig. 3D). We also observed mitotic division in some of the hepatocytes as well as thickening of the hepatocytic plates (Fig. 3A-C).

Kidney morphology in GHR-KO and bGHTg mice

While the kidneys of 2-year-old WT mice were surrounded mostly with WAT (Fig. 4A), the kidneys of GHR-KO mice were surrounded by both WAT and BAT (Figure 4B). Furthermore, there were no significant morphological differences between WT mice (Fig. 4A,C) and GHR-KO mice (Fig. 4B,D). We observed well-developed cortices with normal glomeruli, proximal tubules, and distal tubules, and medullary structures were normally developed in both groups of animals.

By contrast, 6-month-old bGHTg animals displayed several morphological changes within the kidney cortex (Fig. 4F-H) compared with control animals of similar age (Fig. 4E). In the external layer of Bowman’s capsule, we observed a transformation from squamous to

cuboidal epithelium (Fig. 4F,H), while in the proximal tubule, we observed a transformation from simple to stratified epithelium. In bGHTg mice, we also observed signs of glomerulosclerosis (Fig. 4H) and leukocyte infiltration in proximity to damaged glomeruli (Fig. 4F,G). However, no changes were observed in kidney medullar tissue.

Morphology of bone marrow in GHR-KO and bGHTg mice

The bone marrow sections of femora in 2-year-old WT mice and 2-year-old Laron mice revealed a normal structure of the bone marrow (BM) cavities (data not shown). Hematopoietic cords were well developed and single adipocytes, megakaryocytes, numerous macrophages containing hemosiderin, and several proliferating cells with mitotic figures were visible. The sinusoids located between hematopoietic cells contained erythrocytes and leukocytes. Similarly, there were also no significant differences in BM morphology between 6-month-old WT and bGHTg mice, except higher numbers of megakaryocytes were present in the BM hematopoietic cords in bGHTg mice (data not shown).

Spleen morphology in GHR-KO and bGHTg mice

The spleens of 2-year-old WT (Fig. 5C), GHR-KO (Fig. 5D), 6-month-old WT (Fig. 5G), and bGHTg (Fig. 5H) mice were normal. White and red pulp were present, and numerous cells were packed with hemosiderin granules. The only visible difference was for megakaryocytes, which were reduced in number in spleen sections of 2-year-old GHR-KO mice compared with WT animals (Fig. 5C,D) and elevated in number in spleen sections of 6-month-old bGHTg mice compared with 6-month-old WT animals (Fig. 5G,H).

Bone densitometry in GHR-KO and bGHTg mice

Bone densitometry demonstrated an increase of trabecular bone volume in the bGHTg animals compared to WT controls (Fig. 6A). Cortical bone analysis showed similar patterns as total trabecular volume in which GHR-Tg animals had an increased cortical bone volume when compared to WT controls (Fig. 6B). Moreover, GHR-Tg animals exhibited an increased bone mineral density (BMD) when compared to WT animals (Figure 6C).

Discussion

We evaluated the effects of IGF-1 plasma levels on the morphology of major organs since somatotrophic/insulin signaling affects lifespan in experimental animals (reviewed in Piper et al., 2008; Kenyon, 2010), by employing 2-year-old growth hormone receptor knockout (GHR-KO) Laron dwarf mice (with low circulating plasma levels of IGF-1) and 6-month-old bovine growth hormone transgenic (bGHTg) mice (with high circulating plasma levels of IGF-1). In parallel, we analyzed age-matched WT control animals. The ages of the mutant strains employed in our studies were selected based on their overall ~50% survival (Laron dwarf mice live up to ~4 years and bGHTg mice up to ~1 year) (Bartke et al., 2002).

It is well known that there are morphological features of aging, and these are found in the reproductive system (ovaries and testes) as well as in liver and the adipose tissue surrounding vital organs (Maronpot et al., 1999; Ghosh et al., 2012; Hemmeryckx et al., 2012). While morphological changes in female gonads of these mutant mice have already

been reported by our team (Sluczanowska-Glabowska et al., 2012), in this work we focused on morphological changes in lung, heart, liver, kidney, bone marrow, spleen, and bone of WT, GHR-KO, and bGHTg mice.

As expected, we observed differences in liver morphology between animal groups employed in our studies. First, we observed that the livers of long-living GHR-KO animals compared with age-matched WT mice have smaller numbers of cells storing lipids, and the lipid vacuoles within the cells were much smaller (microvesicles). To explain the difference between GHR-KO and WT mice, it is well known that mild steatosis without inflammatory processes may occur spontaneously with advanced age in mice (Maronpot et al., 1999). There may also be an increase in nuclear volume as a result of an increase in chromosome number (polyploid nuclei) (Gregg et al., 2012). Thus, the lower density and smaller sizes of lipid vacuoles observed in Laron mice liver may reflect the better overall health status of these animals.

By contrast, hepatocytes in short-living bGHTg mice were hypertrophic, with enlarged nuclei, and contained more glycogen- and fat-storing granula, and the nuclei in many of these cells were abnormal. As animals were not infected and given standard chow, the steatosis observed in these mice was related to GH/IGF-1-directed accelerated aging. Furthermore, since the marked steatosis is highly connected to insulin resistance, which with time leads to metabolic syndrome and type II diabetes (Merat et al., 2010; Bulum et al., 2011), the high content of lipid-storing cells in bGHTg mice may explain the insulin resistance observed in these mice.

The intranuclear inclusions noted in the hepatocytes of bGHTg mice were also observed by Gregg et al. in a murine model of progyria (*Ercc1*$^{-/\Delta}$ mice), with inherited defects in DNA repair. In these mice, similar PAS-positive inclusions in the nuclei of hepatocytes, lipofuscin-storing cells, liver steatosis, and other features of accelerated aging were described (Gregg et al., 2012). In bGHTg mice, we also detected massive leukocyte infiltration, which has been described as one of the indicators of aging (Maronpot, 1999; Singh et al., 2008; Gregg et al., 2012). However, what was somewhat surprising, we observed hepatocytes at various stages of mitotic division. It is very likely that chronic GH exposure leads to regenerative hyperplasia, apoptosis, or even liver cancer due to the increasing frequency of mitosis in liver or the prolonged expression of GH (Snibson, 2002). These types of changes were observed in different mouse mutants overexpressing GH (e.g., ovine GH) and were described as preneoplastic changes, leading to the development of cancers by the age of 12 months (Snibson, 2002). Thus, bGHTg mice display several preneoplastic changes that may lead to the development of liver malignancies. In fact, the bGHTg mice employed in our studies also developed liver malignancies with advanced age (not published).

Another morphological feature that is often connected with aging is replacement of BAT by WAT around vital organs. In younger animals, most of the adipose tissue surrounding vital organs is composed of BAT, which contains adipocytes filled with numerous small lipid droplets and a high density of mitochondria. In older animals WAT contains adipocytes that each contain one large lipid vacuole. In young laboratory rodents, brown adipose tissue is

found in clusters in specific regions (e.g., the interscapular region, the region surrounding the aorta and kidney, or the intercostal region) (Cousin et al., 1992; Schulz et al., 2011). Since BAT is highly vascularized, it supplies heat to vital organs of the thorax and nervous system (Cannon and Nedergaard, 2004).

During aging, BAT is gradually replaced by WAT (Maronpot et al., 1999). Interestingly, in our experiment we noted a decelerated transformation of the BAT into WAT in GHR-KO mice and accelerated replacement of BAT by WAT in bGHTg animals in regions surrounding the aorta and kidney. In addition, we observed less lymphocytic infiltration in adipose tissue in GHR-KO mice compared with WT age-matched control littermates. A higher content of BAT and less infiltration of adipose tissue by inflammatory cells positively correlates in mice with longevity and protects them from insulin resistance (reviewed in Mattson, 2010; Wu and Meydani, 2008).

As expected because of anabolic activity of GH – we observed in bGHTg mice increase of trabecular bone an increased bone mineral density (BMD) when compared to WT animals. Furthermore, our analysis of BM and spleen tissue did not reveal significant differences between experimental groups, except for an increase in the number of megakaryocytes in bGHTg mice and a slightly lower number in GH-RKO animals compared with the number in age-matched WT mice. This could be easily explained by the well-known effect of GH and IGF-1 on increasing proliferation of megakaryocytes (Blazar et al., 1995). However, while our studies did not discover significant changes in BM morphology, FACS-based measurements of very small embryonic-like stem cells (VSELs) showed a higher number of these primitive stem cells in the BM of GHR-KO mice and a reduced number in bGHTg animals compared with age-matched WT controls (Ratajczak et al., 2011). Changes in the number of VSELs correlated positively in that study with overall changes in the numbers of hematopoietic stem cells and clonogenic progenitors (Ratajczak et al., 2011). These changes however, may not immediately affect morphology of the BM and spleen tissue. Another interesting observation in our current and previous study is that despite significant increase trabecular bone and bone density bGHTg mice have as previously shown a reduced number of most primitive Sca-1^{+}Lin^{-}CD45^{-}hematopoietic stem cells (Ratajczak et al., 2011).

Furthermore, while we observed some changes in the kidneys of bGHTg males, it is most likely that these changes are the effect of extensive GH signaling rather than the aging process itself. The most striking morphological changes observed in these mice were glomerulosclerosis and glomerular hypertrophy, which have also been described in acromegalic patients (reviewed in Grunenwald et al., 2011). In addition to glomerulosclerosis and a transformation from simple to stratified epithelium in proximal tubules, we observed hypertrophy of Bowman's capsule. Similar changes have also been described by Coschigano et al. in 12-month-old bGHTg mice (Coschigano et al., 2010). What is novel is that our data indicate that this process has already occurred in 6-month-old bGHTg animals. Moreover, while glomerulosclerosis is due to an increasing accumulation of collagen types I, III, and IV and fibronectin extracellular mezangial matrix, the hypertrophy and epithelial cell transformations are consequences of direct GH action on renal tissue, and this action cannot be connected to aging (Qian et al., 2008).

In conclusion, our morphological analysis of the organs of long-living 2-year-old Laron dwarf mice (which had reached ~50% of their maximal life span) revealed a lower biological age for its organs, with more brown adipose tissue (BAT) surrounding the main body organs, lower levels of steatosis in liver, and a lower incidence of leukocyte infiltration compared with normal littermates. By contrast, the organs of 6-month-old short-living bGHTg mice display several abnormalities in liver and kidney, which may lead to several age-related complications.

Acknowledgments

This paper was supported with UE structural funds, Innovative Economy Operational Program POIG. 01.01.02-00-109/09 and 2011/02/A/NZ4/00035 Maestro

References

Bartke A. Insulin and aging. Cell Cycle. 2008; 7:3338–3343. [PubMed: 18948730]

Bartke A, Chandrashekar V, Bailey B, Zaczek D, Turyn D. Concequences of growth hormone (GH) overexpression and GH resistance. Neuropeptides. 2002; 36:201–208. [PubMed: 12359510]

Blazar BR, Brennan CA, Broxmeyer HE, Shultz LD, Vallera DA. Transgenic mice expressing either bovine growth hormone (bGH) or human GH releasing hormone (hGRH) have increased splenic progenitor cell colony formation and DNA synthesis in vitro and in vivo. Exp. Hematol. 1995; 23:1397–1406. [PubMed: 7498369]

Brunt EM, Tiniakos DG. Histopathology of nonalcoholic fatty liver disease. World J. Gastroenterol. 2010; 16:5286–5296. [PubMed: 21072891]

Bulum T, Kolariç B, Duvnjak L, Duvnjak M. Nonalcoholic Fatty Liver Disease Markers Are Associated with Insulin Resistance in Type 1 Diabetes. Dig. Dis. Sci. 2011; 56:3655–3663. [PubMed: 21735081]

Cannon B, Nedergaard J. Brown adipose tissue: function and physiological significance. Physiol. Rev. 2004; 84:277–359. [PubMed: 14715917]

Clayton PE, Banerjee I, Murray PG, Renehan AG. Growth hormone, the insulin-like growth factor axis, insulin and cancer risk. Nat. Rev. Endocrinol. 2011; 7:11–24. [PubMed: 20956999]

Coschigano KT, Wetzel AN, Obichere N, Sharma A, Lee S, Rasch R, Guigneaux MM, Flyvbjerg A, Wood TG, Kopchick JJ. Identification of differentially expressed genes in the kidneys of growth hormone transgenic mice. Growth Horm. IGF Res. 2010; 20:345–355. [PubMed: 20655258]

Cousin B, Cinti S, Morroni M, Raimbault S, Ricquier D, Pénicaud L, Casteilla L. Occurrence of brown adipocytes in rat white adipose tissue: molecular and morphological characterization. J. Cell. Sci. 1992; 103:931–942. [PubMed: 1362571]

Flurkey K, Papaconstantinou J, Miller RA, Harrison DE. Lifespan extension and delayed immune and collagen aging in mutant mice with defects in growth hormone production. Proc. Natl. Acad. Sci. USA. 2001; 98:6736–6741. [PubMed: 11371619]

Fontana L, Weiss EP, Villareal DT, Klein S, Holloszy JO. Long-term effects of calorie or protein restriction on serum IGF-1 and IGFBP-3 concentration in humans. Aging Cell. 2008; 7:681–687. [PubMed: 18843793]

Gesing A, Bartke A, Wang F, Karbownik-Lewinska M, Masternak MM. Key regulators of mitochondrial biogenesis are increased in kidneys of growth hormone receptor knockout (GHRKO) mice. Cell Biochem. Funct. 2011; 66:459–467. [PubMed: 21755522]

Ghosh PM, Shu ZJ, Zhu B, Lu Z, Barnes JL, Yeh CK, Zhang BX, Katz MS, Kamat A. Role of ß-adrenic receptors in regulation of hepatic fat accumulation during aging. J. Endocrinol. 2012; 213:251–261. [PubMed: 22457517]

Gregg SQ, Gutiérrez V, Rasile Robinson A, Woodell T, Nakao A, Ross MA, Michalopoulos GK, Rigatti L, Rothermel CE, Kamileri I, Garinis GA, Beer Stolz D, Niedernhofer LJ. A mouse model of accelerated liver aging caused by a defect in DNA repair. Hepatology. 2012; 55:609–621. [PubMed: 21953681]

Grunenwald S, Tack I, Chauvaeau D, Bennet A, Caron P. Impact of growth hormone hypersecretion on the adult human kidney. Ann. Endocrinol. (Paris). 2011; 71:485–495. [PubMed: 22098791]

Harper JM, Salmon AB, Leiser SF, Galecki AT, Miller RA. Skin-derived fibroblasts from long-lived species are resistant to some, but not all, lethal stresses and to the mitochondrial inhibitor rotenone. Aging Cell. 2007; 6:1–13. [PubMed: 17156084]

Hemmeryckx B, Hoylaerts MF, Lijenen HR. Effect of premature aging on murine adipose tissue. Exp. Gerontol. 2012; 47:256–262. [PubMed: 22265801]

Ikeno Y, Hubbard GB, Lee S, Cortez LA, Lew CM, Webb CR, Berryman DE, List EO, Kopchick JJ, Bartke A. Reduced incidence and delayed occurrence of fatal neoplastic diseases in growth hormone receptor/binding protein knockout mice. J. Gerontol. A. Biol. Sci. Med. Sci. 2009; 64:522–529. [PubMed: 19228785]

Kenyon CJ. The genetics of aging. Nature. 2010; 464:504–512. [PubMed: 20336132]

Kinney BA, Coschigano KT, Kopchick JJ, Steger RW, Bartke A. Evidence that age-induced decline in memory retention is delayed in growth hormone resistant GH-R-KO (Laron) mice. Physiol. Behav. 2001; 72:653–660. [PubMed: 11336996]

Kucia M, Masternak M, Liu R, Shin DM, Ratajczak J, Mierzejewska K, Spong A, Kopchick JJ, Bartke A, Ratajczak MZ. The negative effect of prolonged somatotrophic/insulin signaling on an adult bone marrow-residing population of pluripotent very small embryonic-like stem cells (VSELs). Age (Dordr). 2013; 35:315–330. [PubMed: 22218782]

Maronpot, RR.; Boorman, GA.; Gaul, BW. Cache River Press; Vienna. IL: 1999. Pathology of the mouse.

Mattson MP. Perspective: Does brown fat protect against diseases of aging? Aging Res. Rev. 2010; 9:69–76.

McGrane MM, de Vente J, Yun J, Bloom J, Park E, Wynshaw-Boris A, Wagner T, Rottman FM, Hanson RW. Tissue-specific expression and dietary regulation of a chimeric phosphoenolpyruvate carboxykinase/bovine growth hormone gene in transgenic mice. J. Biol. Chem. 1988; 263:11443–11451. [PubMed: 2841327]

Merat S, Khadem-Sameni F, Nouraie M, Derakhshan MH, Tavangar SM, Mossaffa S, Malekzadeh R, Sotoudeh M. A modification of the Brunt system for scoring liver histology of patients with non-Alcoholic Fatty Liver Disease. Arch. Iran Med. 2010; 13:38–44. [PubMed: 20039768]

Miquet JG, González L, Matos MN, Hansen CE, Louis A, Bartke A, Turyn D, Sotelo AI. Transgenic mice overexpressing GH exhibit hepatic upregulation of GH-signaling mediators involved in cell proliferation. J. Endocrinol. 2008; 198:317–330. [PubMed: 18480380]

Olsson B, Bohlooly YM, Brusehed O, Isaksson OG, Ahrén B, Olofsson J, Törnell J. Bovine growth hormone – transgenic mice have major alternations in hepatic expression of metabolic genes. Am. J. Physiol. Endocrinol. Metab. 2003; 285:E504–511. [PubMed: 12736163]

Palmer AJ, Chung MY, List EO, Walker J, Okada S, Kopchick JJ, Berryman DE. Age-related changes in body composition of bovine growth hormone transgenic mice. Endocrinology. 2009; 150:1353–1360. [PubMed: 18948397]

Piper MD, Bartke A. Diet and aging. Cell Metab. 2008; 8:99–104. [PubMed: 18680711]

Piper MDW, Selman C, McElwee JJ, Partridge L. Separating cause from effect: how does insulin/IGF signaling control lifespan in worms, flies and mice? J. Intern. Med. 2008; 263:179–191. [PubMed: 18226095]

Qian Y, Feldman E, Pennathur S, Kretzler M, Brosius FC 3rd. From fibrosis to sclerosis: mechanisms of glomerulosclerosis in diabetic nephropathy. Diabetes. 2008; 57:1439–1445. [PubMed: 18511444]

Ratajczak J, Shin DM, Wan W, Liu R, Masternak MM, Piotrowska K, Wiszniewska B, Kucia M, Bartke A, Ratajczak MZ. Higher number of stem cells in the bone marrow of circulating low Igf-1 level Laron dwarf mice-novel view on Igf-1, stem cells and aging. Leukemia. 2011; 25:729–733. [PubMed: 21233833]

Salmon AB, Murakami S, Bartke A, Kopchick J, Yasumura K, Miller RA. Fibroblast cell lines from young adult mice of long-lived mutant strains are resistant to multiple forms of stress. Am. J. Physiol. Endocrinol. Metab. 2005; 289:E23–29. [PubMed: 15701676]

Schulz TJ, Huang TL, Tran TT, Zhang H, Townsend KL, Shadrach JL, Cerletti M, McDougall LE, Giorgadze N, Tchkonia T, Schrier D, Falb D, Kirkland JL, Wagers AJ, Tseng YH. Identification of inducible brown adipocyte progenitors residing in skeletal muscle and white fat. Proc. Natl. Acad. Sci. USA. 2011; 108:143–148. [PubMed: 21173238]

Singh P, Coskun ZZ, Goode C, Dean A, Thompson-Snipes L, Darlington G. Lymphoid neogenesis and immune infiltration in aged liver. Hepatology. 2008; 47:1680–1690. [PubMed: 18395842]

Sluczanowska-Glabowska S, Laszczynska M, Piotrowska K, Glabowski W, Kopchick JJ, Bartke A, Kucia M, Ratajczak MZ. Morphology of ovaries in laron dwarf mice, with low circulating plasma levels of insulin-like growth factor-1 (IGF-1), and in bovine GH-transgenic mice, with high circulating plasma levels of IGF-1. J. Ovarian Res. 2012; 5:18. [PubMed: 22747742]

Snibson KJ. Hepatocellular kinetics and the expression of growth hormone (GH) in the livers and liver tumors of GH-transgenic mice. Tissue Cell. 2002; 34:88–97. [PubMed: 12165243]

Wu D, Meydani SN. Age-associated changes in immune and inflammatory responses: impact of vitamin E intervention. J. Leukoc. Biol. 2008; 84:900–914. [PubMed: 18596135]

Zhou Y, Xu BC, Maheshwari HG, He L, Reed M, Lozykowski M, Okada S, Cataldo L, Coschigano K, Wagner TE, Baumann G, Kopchick JJ. A mammalian model for Laron syndrome produced by target disruption of the mouse growth hormone receptor/binding protein gene (Laron mouse). Proc. Natl. Acad. Sci. 1997; 94:13215–13220. [PubMed: 9371826]

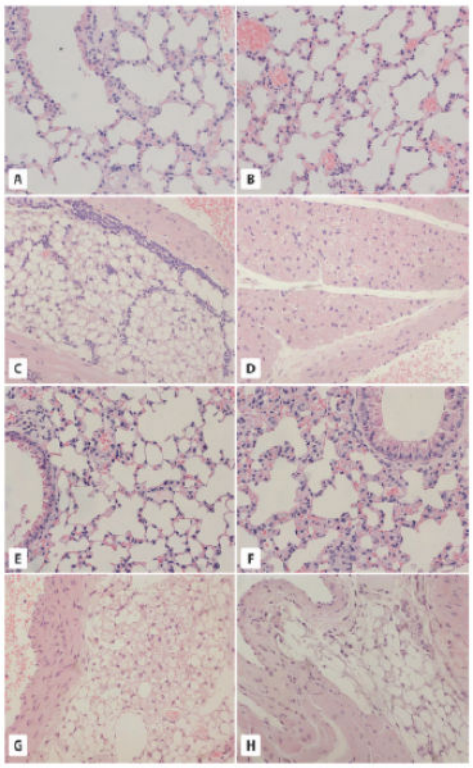

Fig. 1.

The morphology of lung- and aorta-associated adipose tissue in GHR-KO and bGHTg mice. **A and B.** Morphology of the lungs of WT **(A)** and GHR-KO (Laron dwarf) mice **(B)**. The pulmonary alveoli of 2-year-old WT mice and 2-year-old GHR-KO mice show a normal structure of terminal bronchioles and alveoli. **C and D**. Analysis of adipose tissue from the aorta region of WT **(C)** and Laron dwarf mice **(D)**. Adipose tissue sections from 2-year-old WT mice **(C)** reveal the presence of white adipose tissue (WAT) only and leukocyte infiltration. By contrast, 2-year-old GHR-KO mice **(D)** show the presence of brown adipose tissue (BAT) with no leukocyte infiltration. **E and F.** Lung morphology in 6-month-old WT **(C)** and bGHTg **(F)** mice. Both alveoli and terminal bronchioles show normal structure. **G and H.** Analysis of adipose tissue from the aorta region of WT **(G)** and bGHTg **(H)** mice. While the 6-month-old WT mice have both WAT and BAT tissue visible around the aorta **(G)**, the 6-month-old bGHTg mice have WAT with only a few brown adipocytes visible. × 200.

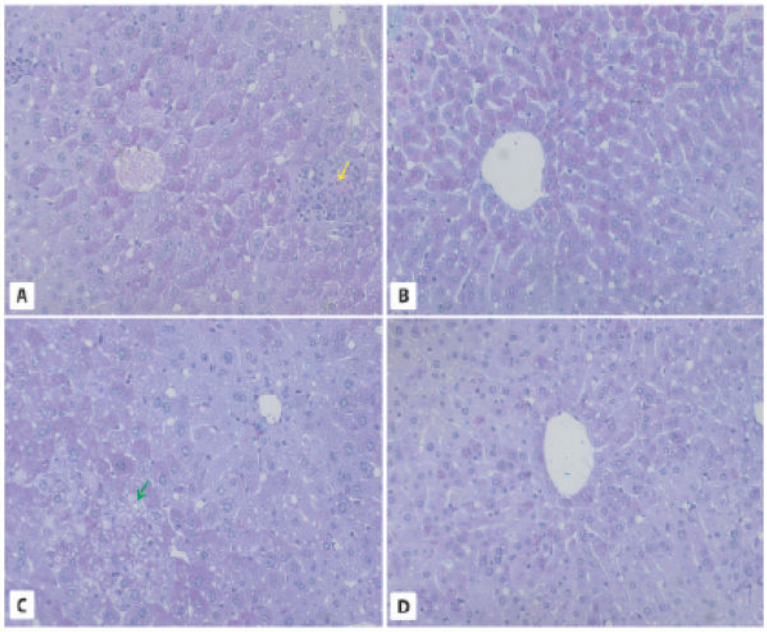

Fig. 2.

Liver morphology in 2-year-old WT and GHR-KO mice. **A, C**. PAS staining of liver sections from WT mice reveals abundant lipid droplets forming macrovesicles (red arrows), fat microvesicles containing ballooning cells, leukocyte infiltrations (yellow arrow), and the presence of hepatocytes with intranuclear inclusions (green arrow). **B, D.** Liver sections in 2-year-old GHR-KO mice show normal morphology. × 200.

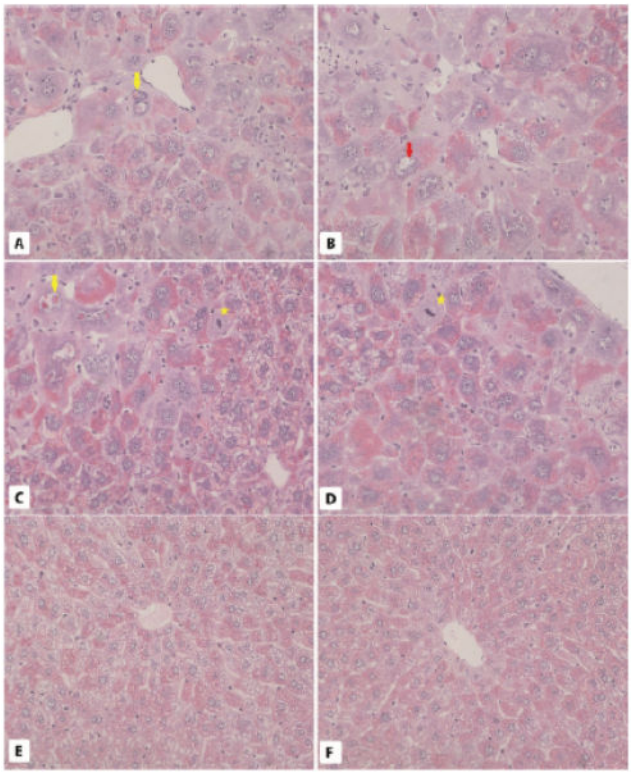

Fig. 3.

Liver morphology in 6-month-old WT and bGHTg mice. **A-D.** PAS staining of liver sections from 6-month-old bGHTg mice reveals the presence of hepatocytes with intranuclear inclusions (yellow arrows), vacuoles (red arrow), and leukocyte infiltration in areas where damaged cells are present (green asterisk). Mitotic figures are also visible (yellow asterisk). **E and F**. Liver sections in 6-month-old WT mouse liver show normal morphology. × 200.

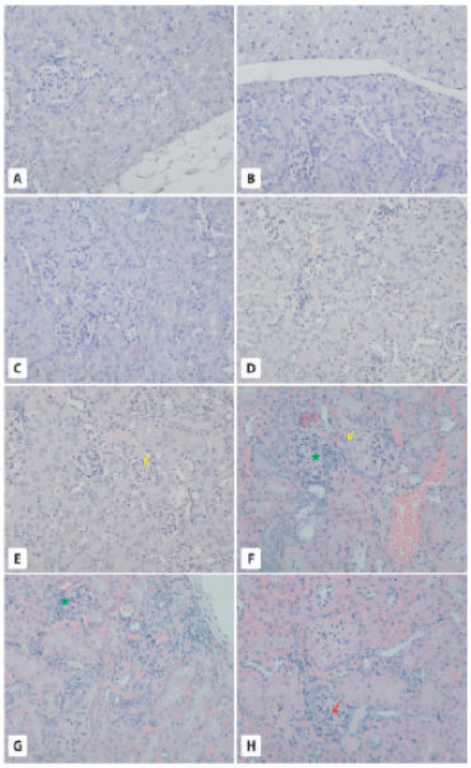

Fig. 4.

Morphology of the kidneys. Panel **A-D.** Two-year-old WT and GHR-KO mice. While kidneys in 2-year-old WT mice are surrounded by WAT **(A)** kidneys in GHR-KO mice are surrounded by both WAT and BAT **(B)**. Overall, kidneys in WT **(C)** and GHR-KO **(D)** mice show normal morphology. **E-H.** Six-month-old WT and bGHTg mice. While 6-month-old WT mice show normal structure for the renal cortex **(E)**, the yellow arrow points to a normal glomerulus), 6-month-old bGHTg mice show several structural changes in kidneys, such as a transformation from simple to stratified epithelium on the outer layer of Bowman's capsule (**F and H**, yellow arrows), leukocyte infiltration (**F**, green asterisk), damaged glomeruli with leukocyte infiltration (**G**, green asterisk) and signs of glomeruosclerosis (**H**, red arrow). × 200.

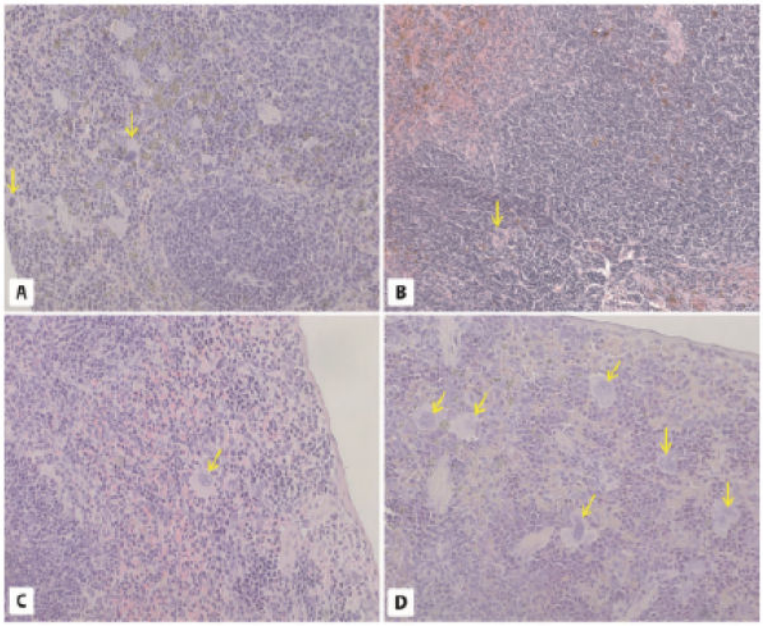

Fig. 5.

Morphology of the spleen. Panels **A-D.** Spleen morphology (H-E staining). The 2-year-old WT **(A)**, GHR-KO **(B)**, 6-month-old WT **(C)**, and 6-month-old bGH TG **(D)** mice show normal spleen morphology. The only visible difference is the increased number of megarkaryocytes (yellow arrows) in the spleens of bGHTg mice **(D)**. × 200.

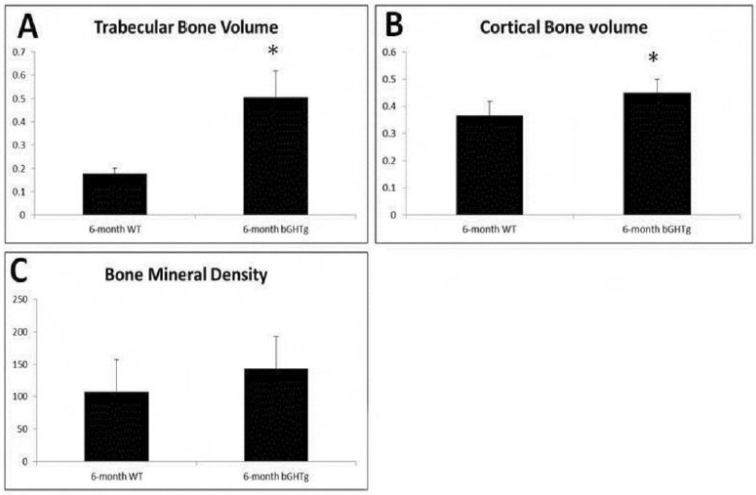

Fig. 6.

Bone densitometry of the humeri of GHR-KO and bGHTg mice. Bone densitometry analysis for 6-month-old WT and 6-month-old bGHTG animals show differences in trabecular bone volume **(A)**, cortical bone volume **(B)**, and bone mineral density (BMD) **(C)**. Visible differences between GHR-Tg animals in trabecular volume, cortical bone volume, and bone mineralized density compared to WT. *P<0.05 compared to WT control.